HHS Public Access

Author manuscript

Int J Radiat Oncol Biol Phys. Author manuscript; available in PMC 2016 January 01.

Published in final edited form as:

Int J Radiat Oncol Biol Phys. 2015 January 1; 91(1): 65–72. doi:10.1016/j.ijrobp.2014.09.008.

Patient-specific quality assurance for the delivery of ^{60}Co intensity modulated radiation therapy subject to a 0.35 T lateral magnetic field

H. Harold Li, PhD, **Vivian L. Rodriguez, PhD**, **Olga L. Green, PhD**, **Yanle Hu, PhD**, **Rojano Kashani, PhD**, **H. Omar Wooten, PhD**, **Deshan Yang, PhD**, and **Sasa Mutic, PhD**

Department of Radiation Oncology, Washington University School of Medicine, 4921 Parkview Place, Campus Box 8224, St. Louis, MO 63110

Abstract

Purpose—This work describes a patient-specific dosimetry quality assurance (QA) program for intensity modulated radiation therapy (IMRT) using ViewRay, the first commercial magnetic resonance imaging guided radiation therapy device.

Methods and materials—The program consisted of the following components: 1) one-dimensional multipoint ionization chamber measurement using a customized 15 cm^3 cubic phantom, 2) two-dimensional (2D) radiographic film measurement using a 30×30×20 cm^3 phantom with multiple inserted ionization chambers, 3) quasi- three-dimensional (3D) diode array (ArcCHECK) measurement with a centrally inserted ionization chamber, 4) 2D fluence verification using machine delivery log files, and 5) 3D Monte-Carlo (MC) dose reconstruction with machine delivery files and phantom CT.

Results—The ionization chamber measurements agreed well with treatment planning system (TPS) computed doses in all phantom geometries where the mean difference (mean ± SD) was 0.0% ± 1.3% (n=102, range, −3.0 % to 2.9%). The film measurements also showed excellent agreement with the TPS computed 2D dose distributions where the mean passing rate using 3% relative/3 mm gamma criteria was 94.6% ± 3.4% (n=30, range, 87.4% to 100%). For ArcCHECK measurements, the mean passing rate using 3% relative/3 mm gamma criteria was 98.9% ± 1.1% (n=34, range, 95.8% to 100%). 2D fluence maps with a resolution of 1×1 mm^2 showed 100% passing rates for all plan deliveries (n=34). The MC reconstructed doses to the phantom agreed well with planned 3D doses where the mean passing rate using 3% absolute/3 mm gamma criteria was 99.0% ± 1.0% (n=18, range, 97.0% to100%), demonstrating the feasibility of evaluating the QA results in the patient geometry.

Corresponding author: H. Harold Li PhD, Department of Radiation Oncology, Washington University School of Medicine, 4921 Parkview Place, Campus Box 8224, St. Louis, MO 63110, Tel: 314-747-9993, Fax: 314-747-9557, hli@radonc.wustl.edu.

Conflict of Interest: None.

Conclusions—We have developed a dosimetry program for ViewRay's patient-specific IMRT QA. The methodology will be useful for other ViewRay users. The QA results presented here can assist the RT community to establish appropriate tolerance and action limits for ViewRay's IMRT QA.

Introduction

The recent clinical integration of a 0.35 T magnetic resonance imaging (MRI) scanner with a ^{60}Co radiation therapy (RT) source, the ViewRay system (ViewRay Inc, Cleveland, OH), provides, for the first time, real-time MRI in the treatment room to guide the treatment delivery (1). In combination with a high-performance treatment planning system (TPS), the ViewRay system's ability to acquire three-dimensional (3D) MR images facilitates online adaptive radiation therapy. Similar to medical linear accelerator (linac) systems, ViewRay offers multiple external-beam radiation therapy options, from very basic open fields to complex intensity modulated radiation therapy (IMRT). As a new technology enters clinical use, patient-specific dosimetry quality assurance (QA) protocols must be explored for individual patient treatments following one-time testing and commissioning of the system (2–5).

ViewRay is a sophisticated RT device with integration of many sub-components, which include the treatment planning system software, its data and algorithms, the information transfer process, the RT delivery system, and the MRI scanner. Compared to conventional linac-based systems, ViewRay is unique in multiple ways. First, the RT delivery is subject to a permanent, lateral magnetic field, the dose deposition perturbation of which has been investigated by several studies (6–9). Meijsing *et al.* (9) demonstrate that the changed trajectories of the secondary electrons due to the Lorentz force have an effect on the dose distribution in a 0.6 cc Farmer chamber's air cavity, and thus on the dose response. This finding may limit the absolute, point measurements to thimble chambers with smaller dimensions, which, on the other hand, are sensitive to positioning inaccuracy in a dose measurement with gradients. The magnetic field may also exclude the use of dosimetry devices that have significant ferromagnetic materials in their design. Second, in order to achieve a dose rate comparable to that of a linac, ViewRay employs three cobalt sources. Due to enhanced Compton-scattering, cobalt sources produce a large number of low-energy scattered photons and thus large variations in scatter-to-primary ratio with changing depth in a phantom (10). This may not be an issue for water-equivalent dosimeters like ionization chamber; however, this may cause calibration problems for the multidimensional dosimeters that are made of non- water-equivalent material either in the detector's active volume or in the surrounding buildup/backscatter medium. Third, each cobalt source has its own double-focused multi-leaf collimators (MLCs) that require precise positioning of each leaf to assure accurate output at the central axis and consistent beam profile and penumbra at the off-axis. (11) For linac- based IMRT QA, MLC positioning validation using machine delivery log files has been reported in multiple publications (12, 13). It is important to implement this method in a ViewRay IMRT QA program in the context of three sets of MLCs and online adaptive RT which ViewRay is designed to support. This implementation is also useful for the QA of non-IMRT fields as electronic portal imaging devices are not necessary on a ViewRay device due to tumor localization using MRI. Finally, there is a clear trend of

moving from gamma passing rates in the phantom geometry to more clinically impactful QA metrics, for instance, dose-volume-histogram (DVH) values in the patient geometry for pretreatment QA (14, 15). ViewRay uses a Monte-Carlo dose computation engine that can be accessed at the treatment console. Owing to efficient variance reduction techniques, a 3D dose calculation can be completed under a minute. Therefore, it is feasible to reconstruct the 3D delivered dose to a phantom using its CT dataset, ultimately a patient's four-dimensional MRI dataset, and the delivery log files immediately after the plan is delivered.

In this manuscript, we describe our experience with patient-specific dosimetry QA for patients receiving IMRT using ViewRay. We demonstrate that the doses delivered in a variety of phantoms, using multiple dosimetry devices, agree with the doses calculated by the TPS within the confidence limits set by the AAPM TG-119 report (3). We also demonstrate that 3D delivered dose to a phantom can be reconstructed in a measurement-based QA session. The limitation of current dosimeters for ViewRay's dosimetry QA is also discussed.

Materials and methods

Treatment planning and delivery

The first 34 patients who received IMRT treatment using a ViewRay RT device at our institution from January 2014 to June 2014 were included in this study. The treatment sites included lung, breast, abdomen, bladder, and rectum. Each patient was imaged using 120-kVp X-ray, slice thickness of 3 mm, and field-of-view of 70 cm using a 64-slice computed tomography scanner. Treatment plans were designed and optimized with ViewRay's TPS version 3.4.1.32 using a Monte-Carlo dose computation algorithm with dose grid resolution of 3×3×3 mm^3. Treatments were delivered using step-and-shoot IMRT technique with ViewRay's three cobalt sources that are 120-degrees apart, each of which is collimated by 30 pairs of doubly-focused MLC leaves that project to 1.05 cm at isocenter.

Multipoint ionization chamber measurement using a 15 cm^3 cubic phantom

Accredited Dosimetry Calibration Laboratory (ADCL) calibrated 0.123 cm^3 cylindrical ionization chambers (Extradin A18, Standard Imaging, Middleton, WI) were used. The standard A18 ionization chamber was modified by the manufacturer to make it compatible with combined MRI/radiation fields. The triaxial cable was replaced with a custom-designed triaxial cable and the metal crimp that secures the clear tube to the chamber stem was replaced with an aluminum crimp so that there were no ferrous materials in its construction. The phantom was composed of a water-equivalent plastic shell that could accept multiple water-equivalent blocks or spacers (Gammex 457, Gammex. Middleton, WI 53562) (16). Ionization chambers can be placed within a 5×5×5 mm^3-spaced grid by using water-equivalent sheets or spacers with different sizes (supplemental Figure e1). Point doses measured with the ionization chamber were compared to point doses calculated by the treatment planning system, which were taken as the mean dose to a 4×4×5 mm^3 region of interest (representing the approximate dimensions of the ionization chamber volume) centered about the midchamber position in the planning CT image set.

2D stacked radiographic film dosimetry using a 30×30×20 cm^3 phantom with multiple inserted ionization chambers

The radiographic film (EDR2, Kodak, Carestream Health, Inc., Rochester NY) measurements were performed by placing the films in the coronal plane in a 30×30×20 cm^3 phantom consisting of 0.5 cm and 1 cm thick plastic sheets (Plastic Water, CNMC, Nashville, TN) (supplemental Figure e2). A film calibration curve was generated to convert the film optical density to dose. An automatic film processor (SRX201A, Konica Minolta Medical Imaging, Wayne, NJ) was used for processing the exposed EDR2 films. The developed films were scanned using a VXR-16 Dosimetry Pro scanner (Vidar Systems Corp., Herndon, VA). The film analysis was carried out using RIT 113 version 5.2 (Radiological Imaging Technology, Inc., Colorado Springs, CO) software. The RIT software was used to register the film to the TPS calculated dose plane. The gamma analysis was performed using the following gamma parameters: relative, global normalization, 3% dose difference threshold, 3 mm DTA threshold, and 10% lower dose threshold.

3D ArcCHECK measurement with a centrally inserted ionization chamber

ArcCHECK (Sun Nuclear Corp., Melbourne, FL) is a cylindrically shaped QA device which is made of PMMA (acrylic) and has an outer diameter of 26.6 cm and an inner cavity diameter of 15.1 cm. 1386 diode detectors of a size of 0.8×0.8 mm^2 are helically arranged at a physical depth of 2.9 cm (water equivalent depth 3.3 g/cm^2) and a detector spacing of 1.0 cm. A MRI-compatible ArcCHECK was used which entailed extending the device's power supply to outside the 5 gauss line. A digital CT dataset of the ArcCHECK device was created with the same dimensions as the physical device, and a uniform relative electron density of 1.125 was applied to all plans recomputed on this dataset. An A18 ionization chamber was positioned at the center of the cavity by a dedicated insert to measure absolute dose simultaneously (supplemental Figure e3). The ArcCHECK software is capable of comparing the measured and planned doses in either relative or absolute modes with global or local dose error thresholds. In this work, ArcCHECK measurements were analyzed using the following gamma parameters: relative, global normalization, 3% dose difference threshold, 3 mm DTA threshold, and 10% lower dose threshold.

Machine delivery file verification

For each delivery, ViewRay's machine delivery log file records MLC leaf positions, beam-on times, gantry angles, and couch positions. The log data are acquired by the treatment delivery system for each radiation field/segment. The record continues until the dynamic treatment is completed or terminated. The analysis of these delivery log files was performed using a MATLAB (The MathWorks, Natick, MA) program that compares delivered to planned parameters. The tolerance was set to 0.5 degrees for gantry, 2 mm for MLC leaf positioning, and 0.2 sec for beam-on time. The program also reconstructs the 2D fluence map with a resolution of 1×1 mm^2 using the as-delivered beam-on-times and MLC positions. The 2D fluence passing rate was defined as the percentage of the pixels with delivery errors less than 2% of the maximum fluence in the field.

3D Monte-Carlo online dose reconstruction with machine delivery file and phantom CT

Using the information recorded in the machine delivery log files and phantom's CT data, 3D delivered dose to the phantom was reconstructed using the on-board Monte-Carlo dose calculation engine. A comparison between reconstructed and planned doses was made using a MATLAB program using the following gamma parameters: absolute, global normalization, 3% dose difference threshold, 3 mm DTA threshold, and 10% lower dose threshold.

Results

Figure 1 shows a histogram of the difference between the ionization chamber measured and TPS calculated point doses. The mean difference was 0.0% ± 1.3% (1 standard deviation, n=102), ranging from −3.0 % to 2.9%. All point-dose measuring results were within 3% of the calculated ones, regardless of which phantom material and which geometry were used. In addition, the ionization chamber showed the same response to a known dose from either a linac or the ViewRay.

Figure 2 shows the typical results for a 2D film analysis using RIT software. [Disease site: stomach; beam angles(°): Group 1: 0; Group 2: 15, 255; Group 3: 30, 150, 270; Group 4: 45, 165, 285; Group 5: 60, 180, 300; Group 6: 75, 195, 315; Group 7: 90, 210, 330; and Group 8: 345]. The film measurement showed excellent agreement with the TPS computed 2D dose distribution. The mean passing rate using relative, 3%/3 mm gamma criteria was 94.6% ± 3.4% (1 standard deviation, n=30), ranging from 87.4% to 100%. Although Low *et al.* (17, 18) state that dose distribution measurement accuracy using 2D radiographic film has not been shown to be better than 5%, stacked film measurement is able to provide a much larger sampling of 3D dose distribution than ionization chamber measurement.

Figure 3 shows the typical results for a 3D ArcCHECK measurement. [Disease site: left adrenal; beam angles (°): Group 1: 80, 200; Group 2: 60, 180; Group 3: 20, 140; Group 4: 40, 160; and Group 5: 225, 345]. The mean passing rate using relative, 3%/3 mm gamma criteria was 98.9% ± 1.1% (1 standard deviation, n=34), ranging from 95.8% to 100%. Kozelka *et al.* (19) report that 3D ArcCHECK has a combined angular and energy dependences of 10%, which can be corrected for by using a virtual inclinometer that relies on one beam being on at a time. Due to the simultaneous delivery of the three cobalt sources, the angular and energy dependences for the ViewRay system were not corrected in this work. As such the ArcCHECK was used as a 3D relative dosimeter, for which a centrally inserted ionization chamber measurement was used to assure the correct normalization which was within 3% for all measurements (cf. Figure 1).

Figure 4 shows the typical results for a machine delivery log file QA (same patient as shown in Figure 2). 2D fluence map showed 100% passing rates for all plan deliveries (n=34). More importantly, ViewRay's fast on-board MC dose calculation engine is able to reconstruct the delivered 3D dose to the patient based on the machine delivery file and phantom CT. The mean passing rate using 3%/3 mm gamma criteria was 99.0% ± 1.0% (1 standard deviation, n=18), ranging from 97.0% to100%. A typical example is shown in Figure 5. [Disease site: bladder; beam angles (°): Group 1: 0; Group 2: 24, 144, 264; Group

3: 48, 168, 288; Group 4: 72, 192, 312; and Group 5: 96, 216, 336]. Note that the gamma failing points lie on two straight lines where the dense, 3-mm thick fiberglass couch structures are located. They are therefore in the dose buildup and builddown regions, which are sensitive to uncertainties in phantom positioning and MC dose computation.

IV. DISCUSSION AND CONCLUSION

This work has adopted a number of experimental and computational dosimetry methods that were developed in the past decade for linac-based IMRT, a result of collaborations between ViewRay, the dosimetry device vendors, and the author's clinical institution. Although dosimetry QA is just part of a multifaceted patient QA program, the results presented here suggests that the delivery of conformal dose distributions using ViewRay in a permanent, 0.35T lateral magnetic field is safe. The dosimetry program has been seamlessly incorporated into the institution's clinical physics program, and it is suggested that the tolerance and action levels recommended by the AAPM be used in a ViewRay patient-specific QA program. The limitations of this program, or rather, the future directions in development, are as follows.

First, due to the three-source nature of the ViewRay, quasi-3D dosimeters (19, 20), for example, ArcCHECK, are ideal for ViewRay's dosimetry measurements. However, the combined field size dependence and angular dependence of an ArcCHECK have been reported to be on the order of 10%. This can be corrected for by using look-up tables as a function of beam angle and field size, for which the beam angle must first be determined using a virtual inclinometer in the ArcCHECK software (19). However, this was not corrected for in this work due to the simultaneous delivery of all three sources. Fortunately, these dependences appeared to partially cancel out in the relative comparison mode, consistently rendering gamma passing rates in the high 90s percent range when using 3%/ 3 mm criteria, but *not* when using tighter tolerances, for example, 2%/2 mm. One possibility to solve this problem is to modify ViewRay's Monte-Carlo code so that the radiation transport in the diodes and surrounding PMMA material can be explicitly simulated. As a result, dose to individual diodes instead of to water can be calculated and subsequently compared to diode's raw response during measurements. By doing this, we can not only convert the ArcCHECK from a relative, 3D dosimeter to an absolute one; more importantly, tighter criteria can be used for the gamma analysis, for example, 2% local dose-error normalization/2 mm instead of 3% global dose-error normalization/3 mm. Nelms *et. al.* (21) have recently made a convincing case that adoption of more sensitive metrics/tighter tolerances enables continual improvement of the accuracy of radiation therapy dose delivery not only at the end user level, but also at the level of product design by the manufacturer. This is especially important for MRI- guided IMRT which is at the early stage of its clinical implementation.

Second, as far as water-equivalence is concerned, the ionization chamber has been the gold standard for single-point, absolute dosimetry. The customized phantoms in this work enable multiple chamber measurements in a single delivery. However, even for three measurement points, it is time consuming to select the dose points in a plan, assemble the box, and manage the cable connections to an electrometer in one QA session. Therefore, a 2D

ionization chamber array is highly desirable. For example, O'Daniel *et. al.* (5) cross-calibrated an ionization chamber array for volumetric-modulated arc therapy QA, and suggested the potential to use the array for both absolute and relative measurements. In order to be relevant for VeiwRay QA, the array device may need to be modified so that it functions properly in a magnetic field. Then angular dependence should be explicitly corrected for to achieve higher measurement precision.

Third, from the multidimensional validation perspective, real 3D water-equivalent dosimeters, for example, PRESAGE (22) and polymer gel dosimeters (23) could play an important role in ViewRay's IMRT QA. Recent development in PRESAGE dosimetry including optical scanner design (22) and dosimeter fabrication, even a deformable dosimeter is under investigation (24), makes this method uniquely suitable for ViewRay dosimetry QA. Meanwhile, as an MRI scanner is readily available in a RT clinic with ViewRay, it may be worthwhile to revisit 3D dosimetry using polymer gel, for example, the BANG gel with the low-field MRI (25, 26).

Finally, several recent publications (27–29) report the use of, for example, low detector-density cylindrical surface dose map from the ArcCHECK to generate a high density, volumetric dose matrix at the phantom or patient's geometry. However, this method relies on the time-resolved dosimeter data with one-beam ON at any given time. One possible solution for ViewRay could be to deliver one beam at a time from a beam group of all 3 beams. The big gain would be the potential to enable patient's DVH-based IMRT QA, while the downside is prolonging the QA time. A future work would be to compare the on-board Monte-Carlo calculated doses to a phantom or a patient after delivery to those reconstructed based on the quasi-3D measurements.

In conclusion, we have developed a dosimetry program for ViewRay's patient-specific IMRT QA. The methodology will be useful for other ViewRay users, and the QA results presented here can assist the RT community to establish appropriate tolerance and action limits for ViewRay's IMRT QA. The challenges in ViewRay dosimetry will open up many research opportunities both in dosimeter design and multi-dimensional dose reconstruction.

Supplementary Material

Refer to Web version on PubMed Central for supplementary material.

Acknowledgments

The authors graciously acknowledge Drs. Iwan Kawrakow and James Dempsey of ViewRay, Inc. for many discussions on this subject. HHL was supported in part by NIH Grant No. R01CA148853.

References

1. Mutic S, Dempsey JF. The ViewRay system: Magnetic resonance–guided and controlled radiotherapy. Seminars in Radiation Oncology. 2014; 24:196–199. [PubMed: 24931092]
2. Kutcher GJ, Coia L, Gillin M, et al. Comprehensive QA for radiation oncology: report of AAPM Radiation Therapy Committee Task Group 40. Med Phys. 1994; 21:581–618. [PubMed: 8058027]

3. Ezzell GA, Burmeister JW, Dogan N, et al. IMRT commissioning: multiple institution planning and dosimetry comparisons, a report from AAPM Task Group 119. Med Phys. 2009; 36:5359–5373. [PubMed: 19994544]
4. Zhu XR, Poenisch F, Song X, et al. Patient-specific quality assurance for prostate cancer patients receiving spot scanning proton therapy using single-field uniform dose. Int J Radiat Oncol Biol Phys. 2011; 81:552–559. [PubMed: 21300457]
5. O'Daniel J, Das S, Wu QJ, et al. Volumetric-modulated arc therapy: effective and efficient end-to-end patient-specific quality assurance. Int J Radiat Oncol Biol Phys. 2012; 82:1567–1574. [PubMed: 21470797]
6. Raaymakers BW, Raaijmakers AJ, Kotte AN, et al. Integrating a MRI scanner with a 6 MV radiotherapy accelerator: dose deposition in a transverse magnetic field. Phys Med Biol. 2004; 49:4109–4118. [PubMed: 15470926]
7. Raaijmakers AJ, Raaymakers BW, Lagendijk JJ. Integrating a MRI scanner with a 6 MV radiotherapy accelerator: dose increase at tissue-air interfaces in a lateral magnetic field due to returning electrons. Phys Med Biol. 2005; 50:1363–1376. [PubMed: 15798329]
8. Kirkby C, Stanescu T, Rathee S, et al. Patient dosimetry for hybrid MRI-radiotherapy systems. Med Phys. 2008; 35:1019–1027. [PubMed: 18404937]
9. Meijsing I, Raaymakers BW, Raaijmakers AJ, et al. Dosimetry for the MRI accelerator: the impact of a magnetic field on the response of a Farmer NE2571 ionization chamber. Phys Med Biol. 2009; 54:2993–3002. [PubMed: 19387100]
10. Wang KK, Zhu TC. Modeling scatter-to-primary dose ratio for megavoltage photon beams. Med Phys. 2010; 37:5270–5278. [PubMed: 21089761]
11. LoSasso T, Chui CS, Ling CC. Physical and dosimetric aspects of a multileaf collimation system used in the dynamic mode for implementing intensity modulated radiotherapy. Med Phys. 1998; 25:1919–1927. [PubMed: 9800699]
12. Stell AM, Li JG, Zeidan OA, et al. An extensive log-file analysis of step-and-shoot intensity modulated radiation therapy segment delivery errors. Med Phys. 2004; 31:1593–1602. [PubMed: 15259664]
13. Rangaraj D, Zhu M, Yang D, et al. Catching errors with patient-specific pretreatment machine log file analysis. Pract Radiat Oncol. 2013; 3:80–90. [PubMed: 24674309]
14. Nelms BE, Zhen H, Tome WA. Per-beam, planar IMRT QA passing rates do not predict clinically relevant patient dose errors. Med Phys. 2011; 38:1037–1044. [PubMed: 21452741]
15. Zhen H, Nelms BE, Tome WA. Moving from gamma passing rates to patient DVH-based QA metrics in pretreatment dose QA. Med Phys. 2011; 38:5477–5489. [PubMed: 21992366]
16. Low DA, Gerber RL, Mutic S, et al. Phantoms for IMRT dose distribution measurement and treatment verification. Int J Radiat Oncol Biol Phys. 1998; 40:1231–1235. [PubMed: 9539580]
17. Low DA, Parikh P, Dempsey JF, et al. Ionization chamber volume averaging effects in dynamic intensity modulated radiation therapy beams. Med Phys. 2003; 30:1706–1711. [PubMed: 12906187]
18. Low DA, Moran JM, Dempsey JF, et al. Dosimetry tools and techniques for IMRT. Med Phys. 2011; 38:1313–1338. [PubMed: 21520843]
19. Kozelka J, Robinson J, Nelms B, et al. Optimizing the accuracy of a helical diode array dosimeter: a comprehensive calibration methodology coupled with a novel virtual inclinometer. Med Phys. 2011; 38:5021–5032. [PubMed: 21978046]
20. Bedford JL, Lee YK, Wai P, et al. Evaluation of the Delta4 phantom for IMRT and VMAT verification. Phys Med Biol. 2009; 54:N167–176. [PubMed: 19384007]
21. Nelms BE, Chan MF, Jarry G, et al. Evaluating IMRT and VMAT dose accuracy: practical examples of failure to detect systematic errors when applying a commonly used metric and action levels. Med Phys. 2013; 40:111722. [PubMed: 24320430]
22. Thomas A, Oldham M. Fast, large field-of-view, telecentric optical-CT scanning system for 3D radiochromic dosimetry. J Phys Conf Ser. 2010; 250:1–5.
23. Baldock C, De Deene Y, Doran S, et al. Polymer gel dosimetry. Phys Med Biol. 2010; 55:R1–63. [PubMed: 20150687]

24. Juang T, Das S, Adamovics J, et al. On the need for comprehensive validation of deformable image registration, investigated with a novel 3-dimensional deformable dosimeter. Int J Radiat Oncol Biol Phys. 2013; 87:414–421. [PubMed: 23886417]
25. Maryanski MJ, Ibbott GS, Eastman P, et al. Radiation therapy dosimetry using magnetic resonance imaging of polymer gels. Med Phys. 1996; 23:699–705. [PubMed: 8724743]
26. Zhang, L.; Du, D.; Green, O., et al. 3D gel dosimetry using ViewRay's on-board MR scanner: a feasibility study. TU-C-BRE-4. AAPM Annual Meeting; 2014;
27. Nelms BE, Opp D, Robinson J, et al. VMAT QA: measurement-guided 4D dose reconstruction on a patient. Med Phys. 2012; 39:4228–4238. [PubMed: 22830756]
28. Feygelman V, Stambaugh C, Opp D, et al. Cross-validation of two commercial methods for volumetric high-resolution dose reconstruction on a phantom for non-coplanar VMAT beams. Radiother Oncol. 2014; 110:558–561. [PubMed: 24440044]
29. Olch AJ. Evaluation of the accuracy of 3DVH software estimates of dose to virtual ion chamber and film in composite IMRT QA. Med Phys. 2012; 39:81–86. [PubMed: 22225277]

The development of a patient-specific IMRT QA program for ViewRay is reported. The results demonstrate that the doses delivered in a variety of phantoms, using multiple MRI-compatible dosimetry devices, agree with the doses calculated by the treatment planning system within the tolerances set by the AAPM TG-119. Further developments are required to be able to evaluate the QA results in the patient geometry using a combination of water-equivalent 3D dosimeters and Monte-Carlo dose reconstruction methods.

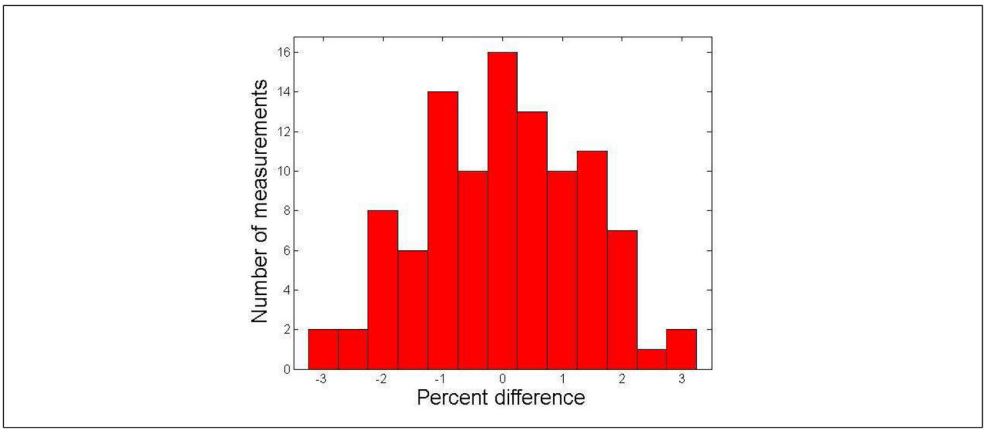

Figure 1.

Histogram of the difference between the ionization chamber measured and TPS calculated point doses. The mean difference was 0.0% ± 1.3% (1 standard deviation, n=102), ranging from −3.0% to 2.9%.

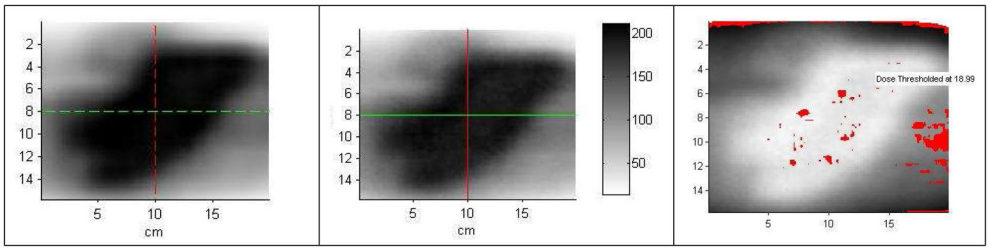

Figure 2.

Typical results for 2D radiographic film measurement vs. TPS. (a) Film measurement; (b) TPS computed dose; (c) Gamma comparison. The points with gamma index greater than 1 are shown in red.

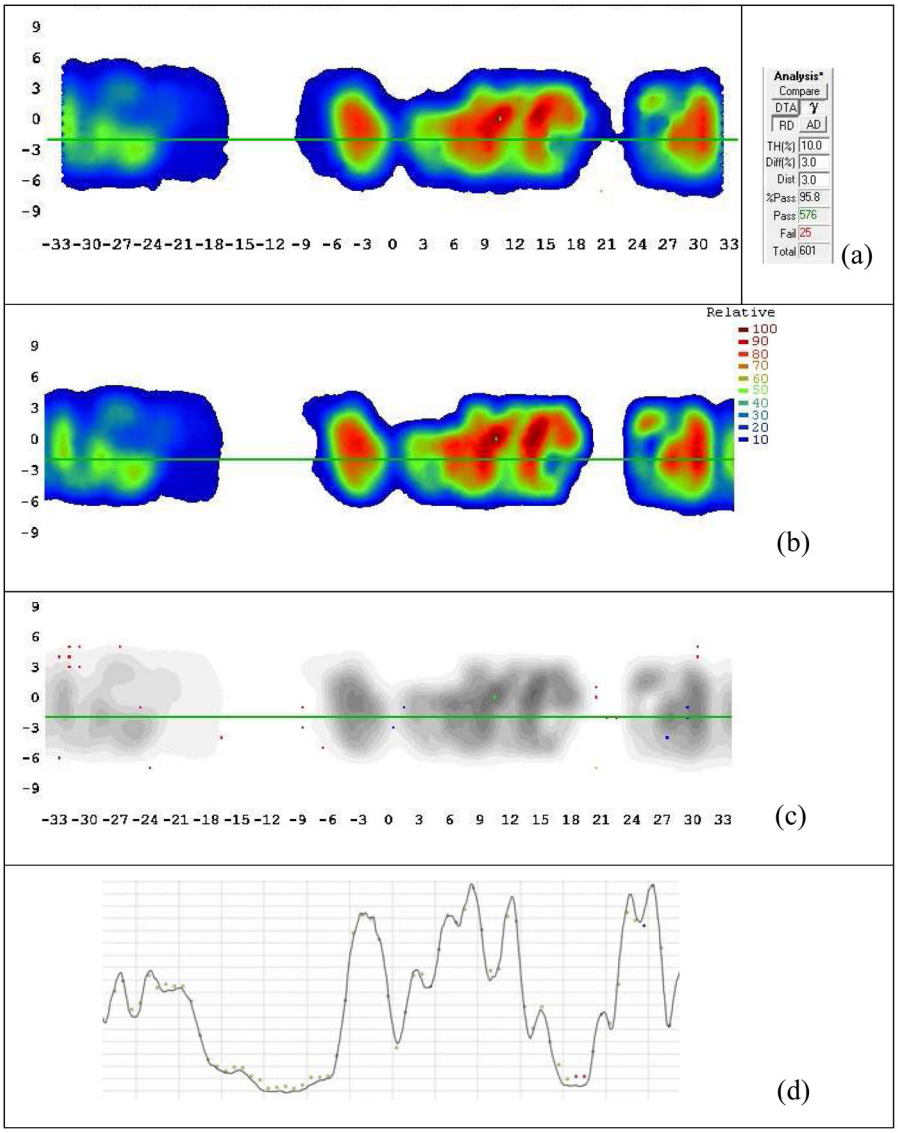

Figure 3.

Typical results for 3D ArcCHECK measurement vs. TPS. (a) ArcCHECK measurement; (b) TPS computed dose; (c) Gamma comparison; (d) Dose profile along the green line shown in (c). The detectors with gamma index greater than 1 are shown in red or blue.

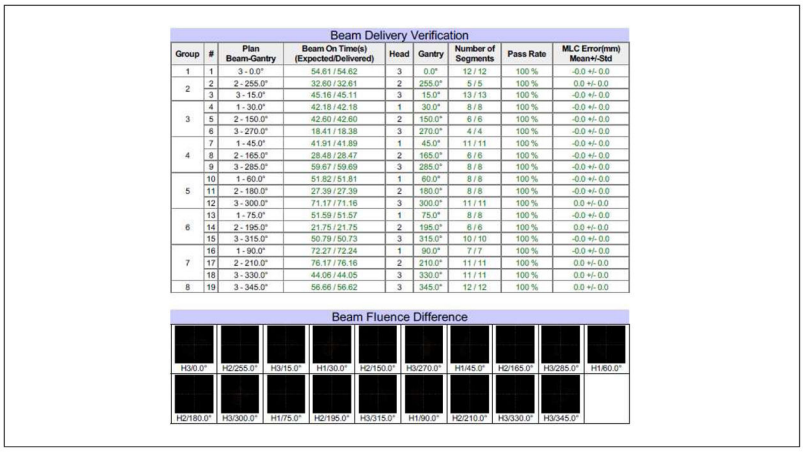

Figure 4.

Typical results for machine delivery log file QA. The tolerance was set to 0.5 degrees for gantry, 2 mm for MLC leaf positioning, and 0.2 sec for beam-on time. The 2D fluence passing rate was defined as the percentage of the pixels with delivery errors less than 2% of the maximum fluence in the field.

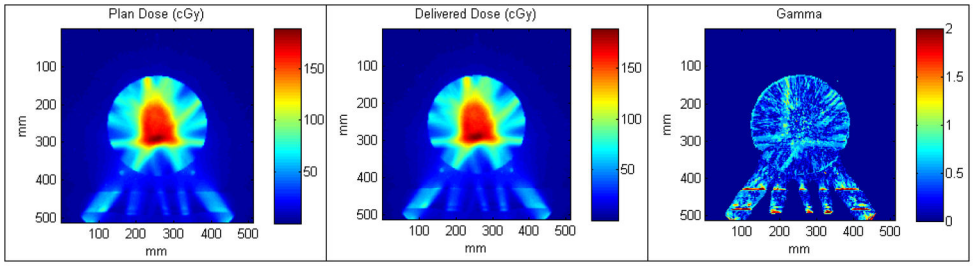

Figure 5.

Typical results for 3D reconstructed dose to an ArcCHECK phantom vs. TPS. (a) Plan dose; (b) Reconstructed 3D dose using machine delivery file; (c) Gamma comparison.